

An updated catalogue of 310 Galactic supernova remnants and their statistical properties

D. A. Green

Astrophysics Group, Cavendish Laboratory, 19 J. J. Thomson Avenue, Cambridge CB3 0HE, United Kingdom

*Corresponding author. E-mail: D.A.Green@mrao.cam.ac.uk

MS received 19 Aug 2024; accepted ?

Abstract. A revised catalogue of 310 Galactic supernova remnants (SNRs) is presented, along with some statistics of their properties. 21 SNRs have been added to the catalogue since the previous published version from 2019, and 5 entries have been removed, as they have been identified as H II regions. Also discussed are some basic statistics of the remnants in the catalogue, the selection effects that apply to the identification of Galactic SNRs and their consequences.

Keywords. supernova remnants — catalogues — ISM: general

1. Introduction

This paper presents the latest version of a catalogue of Galactic supernova remnants (SNRs) which I have compiled for several decades. Previous versions have been published in (Green 1984, 1988, 1991; Stephenson & Green 2002; Green 2004, 2009, 2014, 2019). In addition, more detailed web-based versions of the catalogue have been produced since 1995 which either correspond to one of the published catalogues, or are an intermediate revision. This version of the catalogue contains 310 entries. Section 2 gives the details of the entries in the catalogue, and Section 3 discusses the entries added or removed from the catalogue since the last published version (Green 2019). Section 4 discusses some statistics of the remnants in the current catalogue, the selection effects that apply to the identification of Galactic SNRs, and their consequences.

2. The catalogue format

This catalogue is based on the literature published up to the end of 2023, and contains 310 entries. For each SNR in the catalogue the following parameters are given.

- **Galactic Coordinates** of the remnant. These are quoted to a tenth of a degree, as is conventional. In this catalogue additional leading zeros are not used. These are generally taken from the Galactic coordinate based name used for the remnant in the literature. It should be noted that when these names were first defined, they may not follow the

IAU recommendation¹ that coordinates should be truncated, not rounded to construct such names.

- **Right Ascension and Declination** of J2000.0 equatorial coordinates of the source centroid, for which the accuracy of the quoted values depends on the size of the remnant. For small remnants they are to the nearest few seconds of time and the nearest minute of arc respectively, whereas for larger remnants they are rounded to coarser values, but are in every case sufficient to specify a point within the boundary of the remnant. These coordinates are usually deduced from radio images rather than from X-ray or optical observations.
- **Angular Size** of the remnant, in arcminutes. This is usually taken from the highest resolution radio image available. The boundary of most remnants approximates reasonably well to either a circle or to an ellipse. A single value is quoted for the angular size of the more nearly circular remnants, which is the diameter of a circle with an area equal to that of the remnant. For more elongated remnants the product of two values is given, which are the major and minor diameters of the remnant boundary modelled as an ellipse. In a small number of cases an ellipse is not a good description of the boundary of the object (which will be noted in the description of the object given

¹See: <http://cdsweb.u-strasbg.fr/Dic/iau-spec.htx>.

in its catalogue entry), although an angular size is still quoted for information. For ‘filled-centre’ type remnants (see below), the size quoted is for the largest extent of the observed emission, not, as at times has been used by others, the half-width of the centrally brightened peak.

- **Type** of the SNR: ‘S’ or ‘F’ if the remnant shows a ‘shell’ or ‘filled-centre’ structure, or ‘C’ if it shows ‘composite’ (or ‘combination’) radio structure, with a combination of shell and filled-centre characteristics. If there is some uncertainty, the type is given as ‘S?’, ‘F?’ or ‘C?’, or as ‘?’ in several cases where an object is conventionally regarded as an SNR even though its nature is poorly known or it is not well-understood. (Note: the term ‘composite’ has been used, by some authors, in a different sense, to describe remnants with radio shell and centrally-brightened X-ray emission. An alternative term used to describe such remnants is ‘mixed morphology’, e.g. see [Rho & Petre 1998](#).)
- **Flux Density** of the remnant at a frequency of 1 GHz, in jansky, if available. Not all entries have a value, as some new remnants have not been identified at radio wavelengths, or else the available radio observations are not good enough to provide a reliable flux density. These values are *not* measured values, but are instead derived from the observed radio spectrum of the source. The frequency of 1 GHz is chosen because flux density measurements are usually available at both higher and lower frequencies. Some young remnants – notably G111.7–2.1 (=Cassiopeia A) and G184.6–5.8 (=Crab Nebula) – show secular variations in their radio flux density. In the catalogue the 1-GHz flux densities for G111.7–2.1 and G184.6–5.8 have been taken from ([Perley & Butler 2017](#)), for an epoch of 2016. Results from the primary literature should be used for any detailed quantitative studies of the radio flux densities of these and other remnants.
- **Spectral Index** of the integrated radio emission from the remnant, α (here defined in the sense, $S \propto \nu^{-\alpha}$, where S is the flux density at frequency ν). This is either a value that is quoted in the literature, or one deduced from the available integrated flux densities of the remnant. For several SNRs a simple power law is not adequate to describe their radio spectra, either because there is evidence that the integrated spectrum is curved or the spectral index varies across the face of the remnant. In these cases the spectral index is given

as ‘varies’ (refer to the description of the remnant and appropriate references in the detailed catalogue entry for more information). In some cases, for example where the remnant is highly confused with thermal emission, the spectral index is given as ‘?’ since no value can be deduced with any confidence. These spectral indices have a very wide range of quality, and the primary literature should be consulted for any detailed study of the radio spectral indices of Galactic remnants.

- **Other Names** that are commonly used for the remnant. Note that these are given in parentheses if the remnant is only a part of the source. For some well known remnants – e.g. G184.6–5.8, the Crab Nebula – not all common names are given.

A summary of the data available for all 310 remnants in the catalogue is given in Table 1.

A more detailed version of the catalogue is available on the web². In addition to the basic parameters which are given in Table 1, the detailed version of the catalogue contains the following additional information. (i) Notes on the remnant. For example, if other Galactic coordinates have at times been used to label it (usually before good observations have revealed the full extent of the object, but sometimes in error); if the SNR is thought to be the remnant of a historical SN. (ii) Short descriptions of the observed structure/properties of the remnant at radio, optical and X-ray wavelengths, as appropriate from available observations. (iii) Comments on distance determinations, and any point sources or pulsars in or near the object (although they may not necessarily be related to the remnant). (iv) References to observations are given for each remnant, complete with journal, volume, page, and a short description of what information each paper contains (e.g. for radio observations these generally include the telescopes used, the observing frequencies and resolutions, together with any flux density determinations). These references are *not* complete, but cover recent and representative observations of the remnant that are available, and should themselves include references to earlier work. These references are from the published literature up to the end of 2023, from ‘supernova remnant’ abstract/title/keyword searches on the ‘Astrophysics Data System’³ (ADS).

The detailed version of the catalogue is available in pdf format for downloading and printing, or as web pages, including a page for each individual remnant. The web pages for each remnant include links to ADS

²See: <https://www.mrao.cam.ac.uk/surveys/snrs/>.

³See: <https://ui.adsabs.harvard.edu/>.

for each of the over three thousand references that are included in the detailed listings, and links are also provided for either title/abstract/keyword or full-text searches at ADS by the SNR name(s).

Some of the parameters included in the catalogue are themselves of variable quality. For example, the radio flux density of each remnant at 1 GHz is generally obtained from several radio observations over a range of frequencies, both above and below 1 GHz, so is of good quality. However, there are 27 remnants – often those which have been identified at other than radio wavelengths – for which no reliable radio flux density is yet available, because they have either not been detected or well observed in the radio. Although the detailed version of the catalogue contains notes on distances for many remnants reported in the literature, these are highly variable in terms of reliability and accuracy. Consequently the distances given within the detailed version of catalogue should be used with caution in any statistical studies, and reference should be made to the primary literature cited in the detailed catalogue. For SNR distances, see also [Ranasinghe & Leahy \(2022\)](#), who provide a compilation of distances for 215 Galactic SNRs (although not all of these are included in the catalogue), which are discussed briefly in Section 4.4.

The detailed version of the catalogue also contains notes both on those objects no longer thought to be SNRs, and on the many possible and probable remnants that have been reported in the literature (including possible large, old remnants, seen from radio continuum, X-ray or H I observations). In this revision of the catalogue the detailed version now also includes a list of many of these proposed remnants. See also Section 4.1 below, for discussion of some of the recently proposed remnants.

It should be noted that the catalogue is far from homogeneous. Although many remnants, or possible remnants, were first identified from wide-area radio surveys, there are many others that have been observed with diverse observational parameters. This makes uniform criteria for inclusion in the main catalogue difficult, and the dividing line between entries in the main catalogue and in the list of possible and probable remnants (see Section 4.1) is subjective.

For an alternative catalogue of high-energy observations of Galactic SNRs see [Ferrand & Safi-Harb \(2012\)](#)⁴.

3. Additions and Removals

Since the last published version of the catalogue ([Green 2019](#)), the following SNRs have been added.

- [Hurley-Walker et al. \(2019\)](#) identify several new SNRs, from improved radio observations, which had previously been suggested as candidate remnants by [Gorham \(1990\)](#), [Gray \(1994\)](#), [Duncan et al. \(1995\)](#), [Duncan et al. \(1997\)](#), [Whiteoak & Green \(1996\)](#), [Brogan et al. \(2006\)](#) and [Roberts & Brogan \(2008\)](#), namely: G3.1–0.6, G7.5–1.7, G13.1–0.5, G15.5–0.1, G28.3+0.2, G28.7–0.4, G345.1–0.2, G345.1+0.2, G348.8+1.1, G353.3–1.1 and G359.2–1.1. (Another of the SNRs identified by [Hurley-Walker et al.](#) has been included in the catalogue, as G9.7–0.0, since 2006.)
- G21.8–3.0 identified from radio and other observations by [Gao et al. \(2020\)](#).
- G107.0+9.0, a large ring of optical filaments noted by [Fesen et al. \(2020\)](#), which was subsequently studied at radio wavelengths by [Reich, Gao & Reich \(2021\)](#).
- G249.5+24.5, a large ($\approx 4^\circ$) shell remnant found by [Becker et al. \(2021\)](#) from eROSITA X-ray and other observations.
- G17.8+16.7, a remnant identified from its non-thermal radio emission by [Araya, Hurley-Walker & Quirós-Araya \(2022\)](#).
- [Dokara et al. \(2023\)](#) confirmed three candidate remnants as SNRs, from radio observations, including polarisation (all three of which had been suggested as possible SNRs by [Helfand et al. 2006](#)). Two of these – G28.3+0.2 and G28.7–0.4 – had already been added to the 2022 December web version of catalogue following the observations by [Hurley-Walker et al. \(2019\)](#). The third, G29.3+0.1, has been added to this version of the catalogue.
- A large ($\approx 4^\circ$), high latitude SNR, G116.6–26.1, which was first identified as a possible remnant by [Churazov et al. \(2021\)](#) from X-ray observations, and subsequently confirmed from radio and optical observations ([Churazov et al. 2022](#); [Palaiologou, Leonidaki & Kopsacheili 2022](#)).
- G189.6+3.3, a faint SNR overlapping G189.1+3.0 (=IC443) – first suggested by [Asaoka & Aschenbach \(1994\)](#) from ROSAT

⁴See: <http://snrcat.physics.umanitoba.ca/> for the current version.

X-ray observations – following improved X-ray eROSITA observations by [Camilloni & Becker \(2023\)](#).

- [Gao et al. \(2022\)](#) presented radio observations of two new large SNRs, G203.1+6.6 and G206.7+5.9. These had previously been reported as possible SNRs by both [Reich \(2002\)](#) and [Soberski, Reich & Wielebinski \(2005\)](#).
- One of the candidate remnants reported by [Duncan et al. \(1997\)](#), G288.8–6.3, from radio observations has been confirmed as a large, faint SNR from improved radio observations by [Fili-pović et al. \(2023\)](#).

Note that these include several new remnants identified at high Galactic latitudes. See further discussion in Section 4.3.

In this version of the catalogue 5 objects previously listed as SNRs have been removed.

- G11.1–1.0 and G16.4–0.5, which [Gao et al. \(2019\)](#) identified as H II regions rather than SNRs. ([Gao et al.](#) also identified G20.4+0.1 as an H II region, which had been removed from the catalogue in 2004),
- G8.3–0.0, G10.5–0.0 and G14.3+0.1, which [Dokara et al. \(2021\)](#) identified as H II regions rather than SNRs. ([Dokara et al.](#) also identified G11.1–1.0 as an H II region.)

4. Discussion

4.1 Possible and Probable SNRs

As noted in Section 2, the detailed version of the catalogue includes notes on many objects that have been reported in the literature as possible or probable SNRs. Here I discuss briefly some of the recently proposed SNR candidates.

- [Dokara et al. \(2021\)](#) present radio observations in the region $358^\circ \leq l \leq 60^\circ$, $|b| \leq 1^\circ$, and identify 157 candidate remnants (about half of which are previously proposed candidate SNRs). See further discussion of these in Section 4.3.
- [Sofue \(2020\)](#) identifies a small diameter hole in CO emission as a possible ‘dark’ SNR, a new class of remnant (see also [Sofue 2021](#)).
- [Ritter et al. \(2021\)](#) propose the faint, fast expanding optical nebula Pa 30 as the remnant of

the historical supernova of AD1181, rather than G130.7+3.1 (=3C58). See also [Fesen, Schaefer & Patchick \(2023\)](#); [Lykou et al. \(2023\)](#). However, unlike known young SNRs this has not been detected in the radio (for example see the Canadian Galactic Plane Survey, [Taylor et al. 2003](#)).

4.2 Some Simple Statistics

In the catalogue there are 23 SNRs which do not have a flux density at 1 GHz and 4 with lower limits. This is because either the remnant has not been detected at radio wavelengths, or it is poorly defined by current radio observations, so that their flux density at 1 GHz cannot be determined with any confidence. So 92% of the remnants do have a flux density at 1 GHz in the catalogue. Of the catalogued remnants, $\approx 46\%$ are detected in X-rays, and $\approx 32\%$ in the optical. The smaller proportion of SNR identified in the optical and X-ray wavebands is due to Galactic absorption, which hampers the detection of distant remnants.

In this version of the catalogue, 80% of remnants are classified as shell (or possible shell) remnants, 12% are composite (or possible composite) remnants, and just 3% are filled-centre (or possible filled centre) remnants. The types of the remaining remnants are not clear from current observations (or else they are objects which are conventionally regarded as SNRs although they do not fit well into any of the conventional types, e.g. CTB80 (=G69.0+2.7), MSH 17–39 (=G357.7–0.1)).

4.3 Selection Effects

Previously (e.g. [Green 1991, 2005](#)) I have discussed the selection effects that apply to the identification of Galactic SNRs. Although some SNR are identified first at other than radio wavelengths, most SNRs have been identified first in the radio – and also many remnants are not detected in the optical or in X-rays due to obscuration – and therefore the selection effects for the SNR catalogue are dominated by those that apply at radio wavelengths. These are: (i) the difficulty in identifying low surface brightness remnants the presence of the extended Galactic background, and (ii) the difficulty in recognising small angular size remnants. In [Green \(2005\)](#) I derived a surface brightness completeness limit, at 1 GHz, of $\Sigma_{1\text{ GHz}} \approx 10^{-20} \text{ W m}^{-2} \text{ Hz}^{-1} \text{ sr}^{-1}$. This is based on the Effelsberg 2.7 GHz survey of a large part of the Galactic plane (i.e. $358^\circ < l < 240^\circ$, $|b| < 5^\circ$, see: [Reich et al. 1988, 1990](#); [Fürst et al. 1990](#)). However, the surface brightness completeness limit is likely to be somewhat higher close to the Galactic Centre, where the background Galactic radio emission is brightest, and it is most difficult to identify faint SNRs. Note that sur-

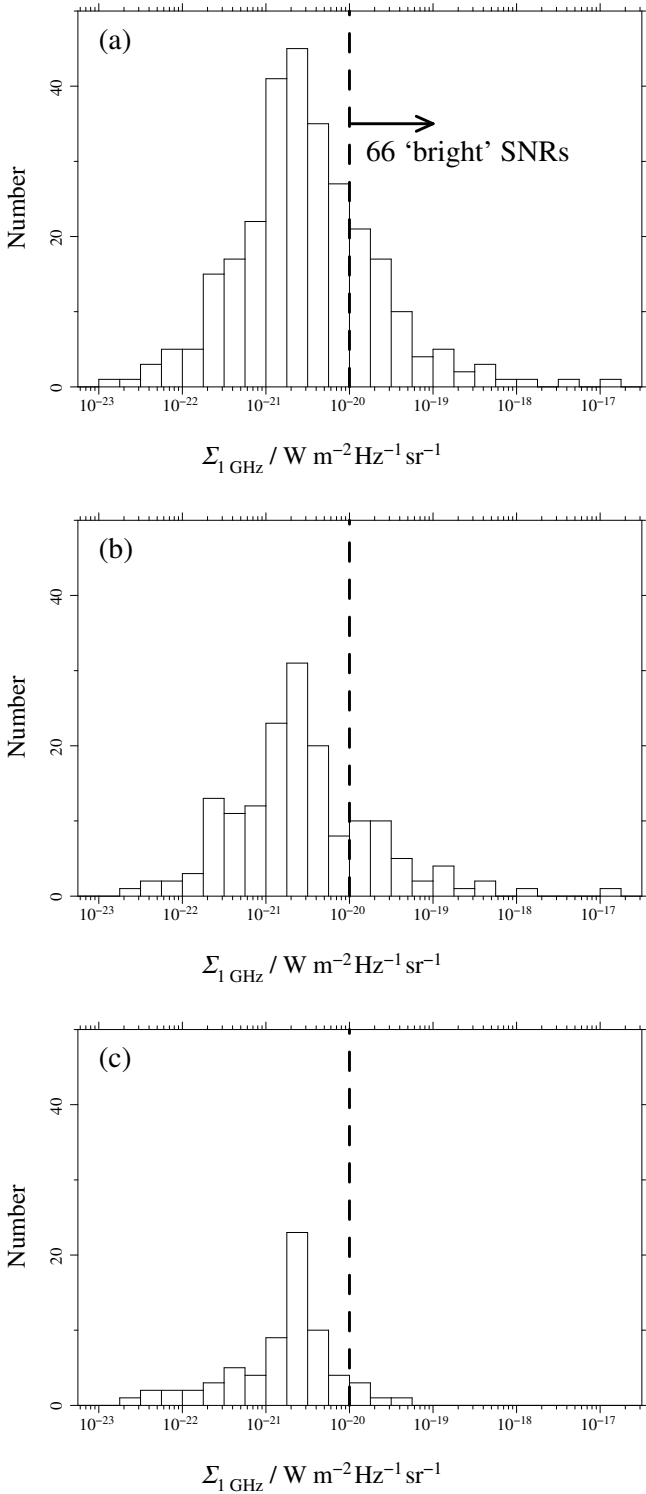


Figure 1. Histograms for the number of SNRs in the current catalogue with surface brightness at 1 GHz: (a) all remnants; (b) remnants in the Effelsberg 2.7-GHz Galactic plane survey region (i.e. $358^\circ < l < 240^\circ$, $|b| < 5^\circ$); (c) remnants in the Effelsberg 2.7-GHz Galactic plane survey region added to the catalogue since 1991.

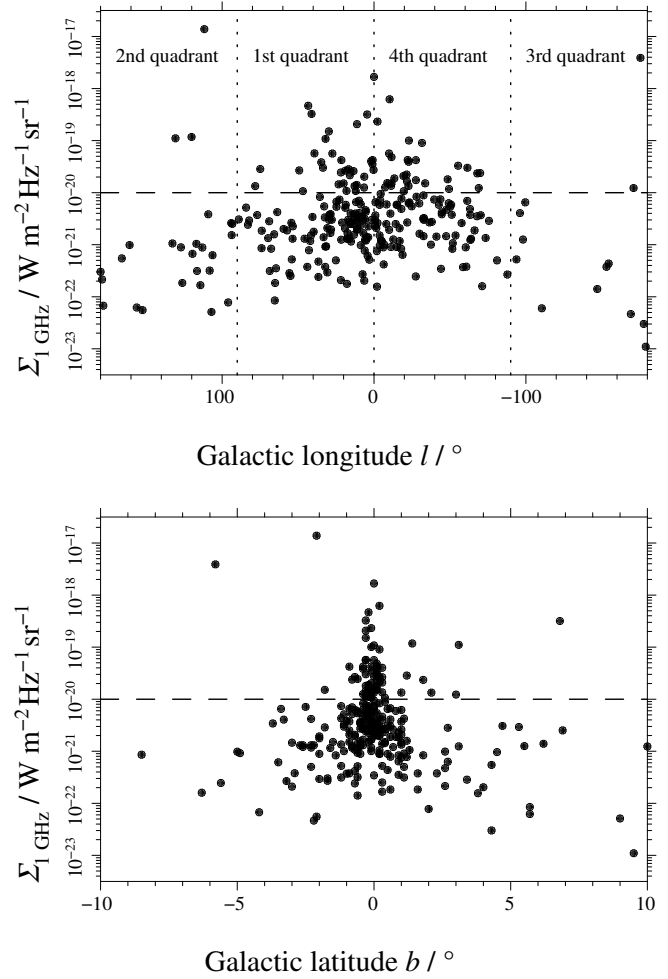


Figure 2. Distribution of SNRs in (top) the $\log \Sigma-l$ and (bottom) $\log \Sigma-b$ planes. All 283 remnants with surface brightnesses are included in the top plot. There are 5 remnants with $|b| > 10^\circ$ not included in the bottom plot.

face brightness is independent of distance. This nominal completeness limit is supported by various searches for SNRs, as no remnants with a surface brightness above this limit have been added to the published versions of the catalogue since Green (2009). This is illustrated in Fig. 1, which shows histograms of SNRs in the catalogue with surface brightness: (a) all 283 with a surface brightness; (b) those in Effelsberg 2.7 GHz survey region, and (c) those in the Effelsberg 2.7 GHz survey region identified since 1991. In the region covered by the Effelsberg 2.7 GHz survey there are 172 remnants (i.e. Fig. 1b), of which 80 have been added to the catalogue since 1991 (i.e. Fig. 1c). The majority of the remnants added after 1991 are below the nominal surface brightness limit of $\approx 10^{-20} \text{ W m}^{-2} \text{ Hz}^{-1} \text{ sr}^{-1}$. The five above the limit are G0.3+0.0, G1.0-0.1, G6.5-0.4, G12.8-0.0 and G18.1-0.1, which are all close to the Galactic Centre. Of these G1.0-0.1 is the brightest,

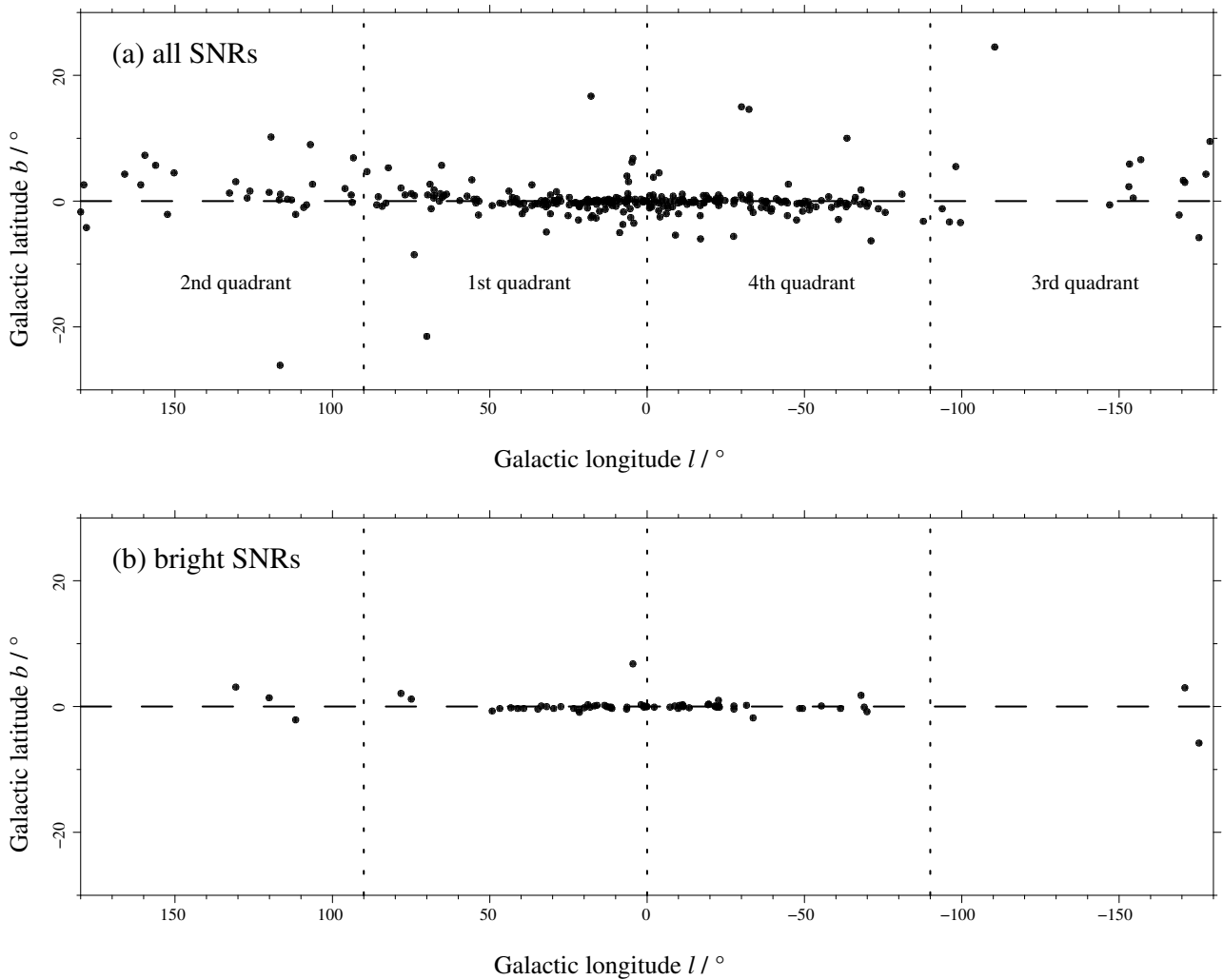


Figure 3. Distribution of SNRs with Galactic latitude and longitude: (top) all remnants; (bottom) the 66 ‘bright’ remnants. Note that the latitude and longitude scales are different.

with $\Sigma_{1\text{ GHz}} \approx 3.5 \times 10^{-20} \text{ W m}^{-2} \text{ Hz}^{-1} \text{ sr}^{-1}$.

This approximate surface brightness limit is consistent with the properties of the 157 SNR candidates reported by Dokara et al. (2021) that were noted in Section 4.1. Flux densities at 5.8 GHz are given for many of these candidates, along with their angular sizes. None of these candidate has a surface brightness above $10^{-20} \text{ W m}^{-2} \text{ Hz}^{-1} \text{ sr}^{-1}$, at 1 GHz (assuming a spectral index of $\alpha = 0.5$).

There are 66 remnants in the current catalogue brighter than the nominal surface brightness completeness limit of $10^{-20} \text{ W m}^{-2} \text{ Hz}^{-1} \text{ sr}^{-1}$. Since it is easier to identify SNRs in regions where the background Galactic emission radio is fainter, i.e. away from $l = 0^\circ$ or $b = 0^\circ$, the distribution of all SNRs in the catalogue is biased towards these regions. This is illustrated in Fig. 2 and 3. Figure 2 shows the distributions of surface brightness with Galactic longitude and latitude. These show

both that faintest identified remnants are in the Galactic anti-centre (i.e. the 2nd and 3rd Galactic quadrants), and at higher Galactic latitudes, and also that a larger proportion of SNRs in these regions are faint. Figure 3 shows the Galactic distribution of all catalogued SNRs and 66 ‘bright’ ones. This shows that distribution of ‘bright’ SNRs are much more concentrated towards the inner Galactic plane (i.e. near $b = 0^\circ$ for the 1st and 4th Galactic quadrants) than that of all catalogue remnants, which gives a biased view of their distribution due to the surface brightness selection effect.

It was noted in Section 3 that in recent years several newly identified SNRs are at relatively high latitude. These include G249.5+24.5 and G116.6–26.1 first identified from eROSITA X-ray observations which are not restricted to the Galactic plane. It is away from the Galactic place where fainter remnants can be more easily identified, which applies not just at radio

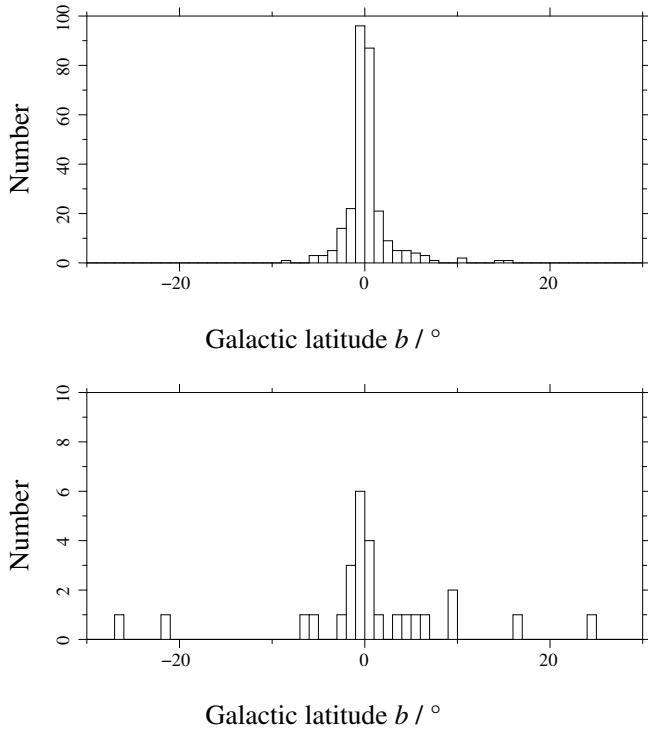


Figure 4. Histograms for the number of SNRs with Galactic latitude: (top) remnants included in the catalogue before 2017 and (bottom) remnants included in the catalogue from 2017 or later. Note that these histograms have different number scales.

wavelengths. Figure 4 shows histograms of SNRs in the catalogue with Galactic latitude, b , for those included in the catalogue in 2017 or earlier, and those added after 2017. For those catalogued in 2017 or earlier 17 of 283 (i.e. 6%) have $|b| \geq 5^\circ$, whereas a much larger proportion of those added after 2017, 10 of 27 (i.e. 37%) have $|b| > 5^\circ$.

The other selection effect that applies is that small angular size remnants – which will be the young but distant SNRs in the Galaxy – need to be resolved, for their structure to be recognised. Most wide field radio surveys have not had good enough resolutions to easily identify small angular size remnants, see Green (2004, 2005) for previous discussion of this.

It is important to note that the surface brightness selection effect is more of a problem towards $l = 0^\circ$ or $b = 0^\circ$. This complicates studies of the properties of Galactic SNRs that also correlate with Galactic coordinates. One example is the distribution of Galactic SNRs with Galactocentric radius, where fainter remnants are easier to identify in the Galactic anti-centre, at large Galactocentric radius. Ranasinghe & Leahy (2022) present studies of the distribution of Galactic SNRs with Galactocentric radius, using a correction factor to deal with selection effects. However, they

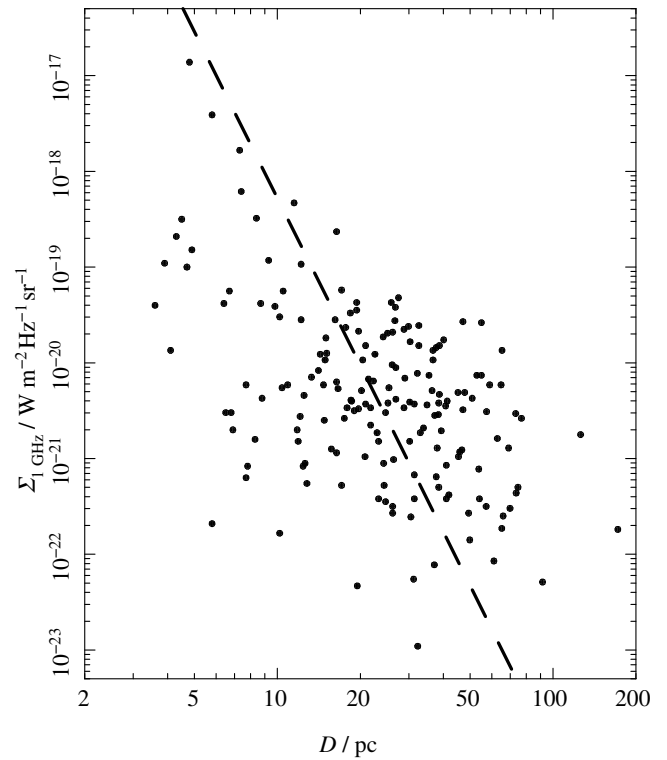


Figure 5. Distribution of 174 remnants with distances, from Ranasinghe & Leahy (2022), in the $\log(\Sigma)$ – $\log(D)$ plane. The dashed line is a least squares fit minimising deviations in $\log(D)$.

assumed this correction depends on the distance from the Sun, which is not correct for the surface brightness selection effect, which is independent of distance. It is more difficult to identify SNRs towards the Galactic centre than it is for SNRs at the same distance towards the Galactic anti-centre, where the Galactic background emission is much fainter. Hence Ranasinghe & Leahy (2022)’s results do not properly take into account the reality of the observational selection effects. See Section 4.5 for further discussion of studies of the distribution of SNRs with Galactocentric radius, using a sample of ‘bright’ SNRs to deal with the surface brightness selection effect. As previously noted, the surface brightness selection effect also correlates with Galactic latitude, which means that faint SNRs are easier to identify a large $|b|$. Hence SNRs at larger distances above or below the Galactic plane are easier to identify, as they are in regions with lower Galactic background emission. Ranasinghe & Leahy (2023) present the distribution of SNRs with height above/below the Galactic plane, but without considering the bias due to the surface brightness selection effect.

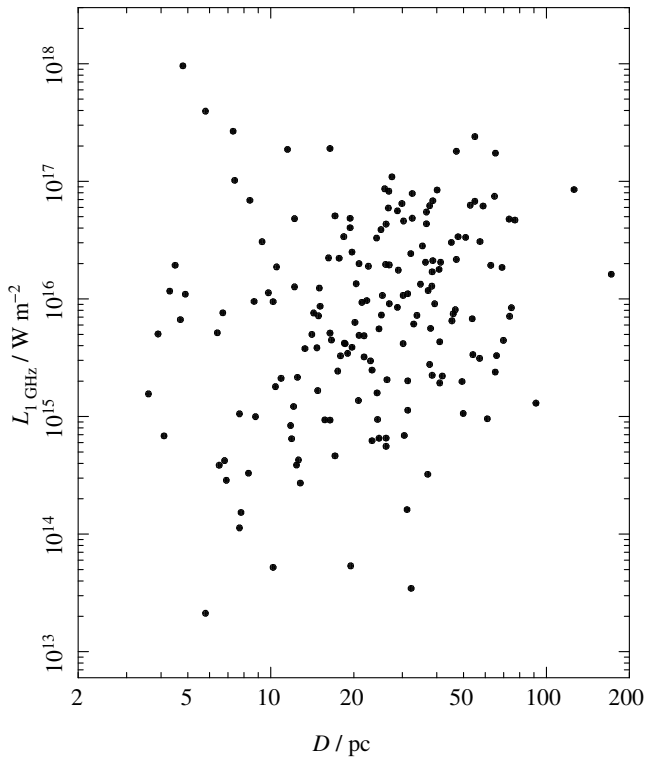


Figure 6. Distribution of 174 remnants with distances, from [Ranasinghe & Leahy \(2022\)](#), in the $\log(L)$ – $\log(D)$ plane.

4.4 ‘ Σ – D ’ relation (and ‘ L – D ’)

As noted above, [Ranasinghe & Leahy \(2022\)](#) provide a compilation of distances for 215 Galactic SNRs. 16 of these are not included in the catalogue, but are included in the possible and probable remnants listed in the detailed version of the catalogue. Of those in the catalogue, several do not have radio flux densities at 1 GHz, giving a sample of 174 SNRs with surface brightness (Σ), distance (d) and physical diameter (D , from d and θ). Although the reliability of the individual distance measurements or estimates are variable, this is a useful large sample of Galactic SNRs with distances. Figure 5 shows the distribution of these 174 remnants in the $\log(\Sigma)$ – $\log(D)$ plane, i.e. the ‘ Σ – D ’ diagram, along with a least square fit straight line fit (which minimises square deviations in $\log(D)$, which is appropriate if it were to be used to estimate D from an observed Σ). This shows that these Galactic SNRs have a wide spread of properties, and hence (as discussed previously, e.g. [Green 1991, 2004](#); [Ranasinghe & Leahy 2023](#)), using the Σ – D fit to obtain a physical diameter, D , for an individual remnant – and hence its distance d via its angular size θ – is very unreliable. Figure 5 shows, for a large range of Σ , a spread of about an order of magnitude in D for a given surface brightness. It should also be remembered that observational selection effects mean that identification of low surface brightness remnants,

and physically small remnants is difficult, so the range of properties of SNRs to the bottom and left of the diagram may not be complete. Figure 5 does show some correlation between surface brightness and physical diameter. However, as I have noted previously (e.g. [Green 2005](#)), much of the correlation is because surface brightness is being plotted against physical diameter. Since $\Sigma \propto S/\theta^2$, and luminosity $L \propto Sd^2$ then $\Sigma \propto L/(\theta d)^2$, or $\Sigma \propto L/D^2$. Thus the Σ – D diagram has a D^{-2} bias compared with a L – D diagram. Figure 6 shows the distribution of the sample of 175 SNRs with distances and flux densities in the $\log(L)$ – $\log(D)$ plane, which does not show any obvious correlation.

4.5 Galactocentric Distribution

As noted in Section 4.3, studies of the distribution of SNRs with Galactocentric radius, R , are complicated by the surface brightness selection effect. An alternative approach is to use a sample of ‘bright’ SNRs, to mitigate this, and then compare their distribution with Galactic longitude with that expected from a model. In [Green \(2015\)](#) I used a sample of 69 SNRs with a surface brightness, at 1 GHz, above $10^{-20} \text{ W m}^{-2} \text{ Hz}^{-1} \text{ sr}^{-1}$, and compared these with a power-law/exponential model distribution of SNRs of the form $(R/R_{\odot})^{\alpha} \exp(-\beta(R - R_{\odot})/R_{\odot})$ (as this is the form used by previous studies, e.g. [Case & Bhattacharya 1998](#)). The best fit parameters produced a distribution that peaked at a smaller Galactocentric radius than the result from [Case & Bhattacharya \(1998\)](#), and hence had a larger fraction of remnants within the Solar circle (77% rather than 49%).

The current catalogue has 66 SNRs above the surface brightness limit of $10^{-20} \text{ W m}^{-2} \text{ Hz}^{-1} \text{ sr}^{-1}$, which is three less than in the sample of ‘bright’ SNRs used by [Green \(2015\)](#). This is because: (i) two objects – G20.4+0.1 and G23.6+0.3 – have since been identified as H II regions not SNRs (see [Anderson et al. 2017](#)), and so have removed from the catalogue, and (ii) more recent radio observations by [Ball et al. \(2023\)](#) for G327.4+0.4 give a slightly lower flux density for it at 1 GHz, so its surface brightness now falls just below $10^{-20} \text{ W m}^{-2} \text{ Hz}^{-1} \text{ sr}^{-1}$. However, changing the sample of ‘bright’ SNRs from 69 to 66 does not change the main results of fitting a power-law/exponential model to the observed distribution of Galactic longitude (i.e. the distribution peaks at a smaller Galactocentric radius with a larger fraction with the Solar circle than obtained by [Case & Bhattacharya](#)).

[Verberne & Vink \(2021\)](#) present a similar study of the Galactocentric distribution of SNRs using a sample of bright remnants, and comparing their distribution in l with than expected from models. They use several different models, not just a power-law/exponential, and use

a slightly higher surface brightness limit, at 1 GHz, of $1.3 \times 10^{-20} \text{ W m}^{-2} \text{ Hz}^{-1} \text{ sr}^{-1}$, which gives a somewhat smaller sample of 57 ‘bright’ remnants. Verberne & Vink prefer a purely exponential decaying distribution of SNRs with Galactocentric radius. Their best fit exponential distribution is more concentrated towards the Galactic centre than the power-law/exponential distribution. The exponential distribution looks quite different from the power-law/exponential distribution, with a peak at $R = 0$. However, when considering the integrated surface density, i.e. density $\times 2\pi R dR$, the exponential result from Verberne & Vink (2021) and the power-law/exponential from Green (2015) are very similar (see figure 5 of Verberne & Vink). It should be remembered that the volume of the Galaxy close to $R = 0$ is small, and the distribution of SNRs here is not well constrained. This is both due to small number statistics, and also the fact that the Galactic background emission is brightest close to $l = 0^\circ$. So, near to $l = 0^\circ$ finding SNRs just above the nominal surface brightness completeness limit is more still difficult, as discussed in Section 4.3. Indeed, even with a slightly higher surface brightness limit, Verberne & Vink (2021) note their sample of bright remnants ‘cannot be assumed to be unbiased’ for $|l| < 10^\circ$.

Finally, it should be remembered that the Galactocentric distributions discussed above are of observed SNRs. This will not be the distribution of Galactic supernovae if the observability SNRs above the radio surface brightness limit depends on some property (e.g. ISM density) which varies with Galactocentric radius.

Acknowledgements

I am grateful to colleagues for numerous comments on, and corrections to the various versions of the Galactic SNR catalogue. This research has made use of the Astrophysics Data System, funded by NASA under Cooperative Agreement 80NSSC21M00561, the SIMBAD database, CDS, Strasbourg Astronomical Observatory, France.

References

Anderson L. D., et al., 2017, *A&A*, 605, A58
 Araya M., Hurley-Walker N., Quirós-Araya S., 2022, *MNRAS*, 510, 2920
 Asaoka I., Aschenbach B., 1994, *A&A*, 284, 573
 Ball B. D., et al., 2023, *MNRAS*, 524, 1396
 Becker W., Hurley-Walker N., Weinberger C., Nicastro L., Mayer M. G. F., Merloni A., Sanders J., 2021, *A&A*, 648, A30

Brogan C. L., Gelfand J. D., Gaensler B. M., Kassim N. E., Lazio T. J. W., 2006, *ApJL*, 639, L25
 Camilloni F., Becker W., 2023, *A&A*, 680, A83
 Case G. L., Bhattacharya D., 1998, *ApJ*, 504, 761
 Churazov E. M., Khabibullin I. I., Bykov A. M., Chugai N. N., Sunyaev R. A., Zinchenko I. I., 2021, *MNRAS*, 507, 971
 Churazov E. M., Khabibullin I. I., Bykov A. M., Chugai N. N., Sunyaev R. A., Zinchenko I. I., 2022, *MNRAS*, 513, L83
 Dokara R., et al., 2021, *A&A*, 651, A86
 Dokara R., et al., 2023, *A&A*, 671, A145
 Duncan A. R., Stewart R. T., Haynes R. F., Jones K. L., 1995, *MNRAS*, 277, 36
 Duncan A. R., Stewart R. T., Haynes R. F., Jones K. L., 1997, *MNRAS*, 287, 722
 Ferrand, G. & Safi-Harb, S., 2012, *A&A*, 49, 1313
 Fesen R. A., et al., 2020, *MNRAS*, 498, 5194
 Fesen R. A., Schaefer B. E., Patchick D., 2023, *ApJL*, 945, L4
 Filipović M. D., et al., 2023, *AJ*, 166, 149
 Fürst E., Reich W., Reich P., Reif K., 1990, *A&AS*, 85, 691
 Gao X. Y., Reich P., Hou L. G., Reich W., Han J. L., 2019, *A&A*, 623, A105
 Gao X. Y., Reich P., Reich W., Hou L. G., Han J. L., 2020, *MNRAS*, 493, 2188
 Gao X., Reich W., Sun X., Zhao H., Hong T., Yuan Z., Reich P., Han J., 2022, *SCPMA*, 65, 129705
 Gorham P. W., 1990, *ApJ*, 364, 187
 Gray A. D., 1994, *MNRAS*, 270, 847
 Green D. A., 1984, *MNRAS*, 209, 449
 Green D. A., 1988, *Ap&SS*, 148, 3
 Green D. A., 1991, *PASP*, 103, 209
 Green D. A., 2004, *BASI*, 32, 335
 Green D. A., 2005, *MmSAI*, 76, 534
 Green D. A., 2009, *BASI*, 37, 45
 Green D. A., 2014, *BASI*, 42, 47
 Green D. A., 2015, *MNRAS*, 454, 1517
 Green D. A., 2019, *JApA*, 40, 36
 Helfand D. J., Becker R. H., White R. L., Fallon A., Tuttle S., 2006, *AJ*, 131, 2525
 Hurley-Walker N., et al., 2019, *PASA*, 36, e048
 Lykou F., Parker Q. A., Ritter A., Zijlstra A. A., Hillier D. J., Guerrero M. A., Le Dû P., 2023, *ApJ*, 944, 120
 Palaiologou E. V., Leonidaki I., Kopsacheili M., 2022, *MNRAS*, 515, 339
 Perley R. A., Butler B. J., 2017, *ApJS*, 230, 7
 Ranasinghe S., Leahy D., 2022, *ApJ*, 940, 63
 Ranasinghe S., Leahy D., 2023, *ApJS*, 265, 53
 Reich W., 2002, in Becker, W., Lesch, H., Trümper, J., eds, *Neutron Stars, Pulsars, and Supernova Remnants*, Max-Planck-Institut für extraterrestrische Physik, p1

- Reich W., Fürst E., Reich P., Junkes N., 1988, in Roger, R. S., Landecker, T.L., *Supernova Remnants and the Interstellar Medium*, IAU Colloquium 101, Cambridge University Press, p293
- Reich W., Fürst E., Reich P., Reif K., 1990, *A&AS*, 85, 633
- Reich W., Gao X., Reich P., 2021, *A&A*, 655, A10
- Rho J., Petre R., 1998, *ApJ*, 503, L167
- Ritter A., Parker Q. A., Lykou F., Zijlstra A. A., Guerrero M. A., Le Dû P., 2021, *ApJL*, 918, L33
- Roberts M. S. E., Brogan C. L., 2008, *ApJ*, 681, 320
- Soberski S., Reich W., Wielebinski R., 2005, *ASPC*, 343, 286
- Sofue Y., 2020, *PASJ*, 72, L11
- Sofue Y., 2021, *Galaxies*, 9, 13
- Stephenson F. R., Green D. A., 2002, *Historical supernovae and their remnants*, Oxford University Press
- Taylor A. R., et al., 2003, *AJ*, 125, 3145
- Verberne S., Vink J., 2021, *MNRAS*, 504, 1536
- Whiteoak J. B. Z., Green A. J., 1996, *A&AS*, 118, 329

Table 1. 310 Galactic supernova remnants: summary data.

l l°	b b°	RA (J2000) /(h m s)	Dec /($^\circ$ ')	size /arcmin	type	Flux at 1 GHz/Jy	spectral index	other name(s)
0.0	+0.0	17 45 44	-29 00	3.5×2.5	S	100?	0.8?	Sgr A East
0.3	+0.0	17 46 15	-28 38	15×8	S	22	0.6	
0.9	+0.1	17 47 21	-28 09	8	C	18?	varies	
1.0	-0.1	17 48 30	-28 09	8	S	15	0.6?	
1.4	-0.1	17 49 39	-27 46	10	S	2?	?	
1.9	+0.3	17 48 45	-27 10	1.5	S	0.6	0.6	
3.1	-0.6	17 55 30	-26 35	52×28	S	5	0.9?	
3.7	-0.2	17 55 26	-25 50	14×11	S	2.3	0.65	
3.8	+0.3	17 52 55	-25 28	18	S?	3?	0.6	
4.2	-3.5	18 08 55	-27 03	28	S	3.2?	0.6?	
4.5	+6.8	17 30 42	-21 29	3	S	19	0.64	Kepler, SN1604, 3C358
4.8	+6.2	17 33 25	-21 34	18	S	3	0.6	
5.2	-2.6	18 07 30	-25 45	18	S	2.6?	0.6?	
5.4	-1.2	18 02 10	-24 54	35	C?	35?	0.2?	Milne 56
5.5	+0.3	17 57 04	-24 00	15×12	S	5.5	0.7	
5.9	+3.1	17 47 20	-22 16	20	S	3.3?	0.4?	
6.1	+0.5	17 57 29	-23 25	18×12	S	4.5	0.9	
6.1	+1.2	17 54 55	-23 05	30×26	F	4.0?	0.3?	
6.4	-0.1	18 00 30	-23 26	48	C	310	varies	W28
6.4	+4.0	17 45 10	-21 22	31	S	1.3?	0.4?	
6.5	-0.4	18 02 11	-23 34	18	S	27	0.6	
7.0	-0.1	18 01 50	-22 54	15	S	2.5?	0.5?	
7.2	+0.2	18 01 07	-22 38	12	S	2.8	0.6	
7.5	-1.7	18 10 00	-23 10	100	S	18?	0.7?	
7.7	-3.7	18 17 25	-24 04	22	S	11	0.32	1814-24
8.7	-5.0	18 24 10	-23 48	26	S	4.4	0.3	
8.7	-0.1	18 05 30	-21 26	45	S?	80	0.5	(W30)
8.9	+0.4	18 03 58	-21 03	24	S	9	0.6	
9.7	-0.0	18 07 22	-20 35	15×11	S	3.7	0.6	
9.8	+0.6	18 05 08	-20 14	12	S	3.9	0.5	
9.9	-0.8	18 10 41	-20 43	12	S	6.7	0.4	
11.0	-0.0	18 10 04	-19 25	11×9	S	1.3	0.6	
11.1	-0.7	18 12 46	-19 38	11×7	S	1.0	0.7	
11.1	+0.1	18 09 47	-19 12	12×10	S	2.3	0.4	
11.2	-0.3	18 11 27	-19 25	4	C	22	0.5	
11.4	-0.1	18 10 47	-19 05	8	S?	6	0.5	
11.8	-0.2	18 12 25	-18 44	4	S	0.7	0.3	
12.0	-0.1	18 12 11	-18 37	7?	?	3.5	0.7	
12.2	+0.3	18 11 17	-18 10	6×5	S	0.8	0.7	
12.5	+0.2	18 12 14	-17 55	6×5	C?	0.6	0.4	
12.7	-0.0	18 13 19	-17 54	6	S	0.8	0.8	
12.8	-0.0	18 13 37	-17 49	3	C?	0.8	0.5	
13.1	-0.5	18 16 00	-17 49	38×28	S	11?	0.6?	
13.3	-1.3	18 19 20	-18 00	70×40	S?	?	?	
13.5	+0.2	18 14 14	-17 12	5×4	S	3.5?	1.0?	
14.1	-0.1	18 16 40	-16 41	6×5	S	0.5	0.6	
15.1	-1.6	18 24 00	-16 34	30×24	S?	5.5?	0.0?	
15.4	+0.1	18 18 02	-15 27	15×14	C?	5.6	0.62	
15.5	-0.1	18 19 25	-15 32	9×8	?	1.2?	0.55?	
15.9	+0.2	18 18 52	-15 02	7×5	S?	5.0	0.63	
16.0	-0.5	18 21 56	-15 14	15×10	S	2.7	0.6	
16.2	-2.7	18 29 40	-16 08	17	S	2.5	0.4	
16.7	+0.1	18 20 56	-14 20	4	C	3.0	0.6	
17.0	-0.0	18 21 57	-14 08	5	S	0.5	0.5	
17.4	-2.3	18 30 55	-14 52	24?	S	5	0.5?	

Table 1. (continued).

l l°	b b°	RA (J2000) /(h m s)	Dec /($^\circ$ ')	size /arcmin	type	Flux at 1 GHz/Jy	spectral index	other name(s)
17.4	-0.1	18 23 08	-13 46	6	S	0.4	0.7	
17.8	-2.6	18 32 50	-14 39	24	S	5	0.5	
17.8	+16.7	17 24 10	-05 10	51×45	S?	2.7	0.8	
18.1	-0.1	18 24 34	-13 11	8	S	4.6	0.5	
18.6	-0.2	18 25 55	-12 50	6	S	1.4	0.4	
18.8	+0.3	18 23 58	-12 23	17×11	S	33	0.46	Kes 67
18.9	-1.1	18 29 50	-12 58	33	C?	37	0.39	
19.1	+0.2	18 24 56	-12 07	27	S	10	0.5	
20.0	-0.2	18 28 07	-11 35	10	F	10	0.1	
21.0	-0.4	18 31 12	-10 47	9×7	S	1.1	0.6	
21.5	-0.9	18 33 33	-10 35	5	C	7	varies	
21.6	-0.8	18 33 40	-10 25	13	S	1.4	0.5?	
21.8	-3.0	18 41 50	-11 16	60	S	5	0.7	
21.8	-0.6	18 32 45	-10 08	20	S	65	0.56	Kes 69
22.7	-0.2	18 33 15	-09 13	26	S?	33	0.6	
23.3	-0.3	18 34 45	-08 48	27	S	70	0.5	W41
24.7	-0.6	18 38 43	-07 32	15?	S?	8	0.5	
24.7	+0.6	18 34 10	-07 05	30×15	C?	20?	0.2?	
25.1	-2.3	18 45 10	-08 00	80×30?	S	8	0.5?	
27.4	+0.0	18 41 19	-04 56	4	S	6	0.68	4C-04.71
27.8	+0.6	18 39 50	-04 24	50×30	F	30	varies	
28.3	+0.2	18 42 30	-03 58	10	S	1.3?	0.7?	
28.6	-0.1	18 43 55	-03 53	13×9	S	3?	?	
28.7	-0.4	18 45 30	-03 54	9	S	0.9?	0.8?	
28.8	+1.5	18 39 00	-02 55	100?	S?	?	0.4?	
29.3	+0.1	18 44 36	-03 06	10?	C?	2.5?	?	
29.6	+0.1	18 44 52	-02 57	5	S	0.5?	0.5?	
29.7	-0.3	18 46 25	-02 59	3	C	9	0.7	Kes 75
30.7	-2.0	18 54 25	-02 54	16	?	0.5?	0.7?	
30.7	+1.0	18 44 00	-01 32	24×18	S?	6	0.4	
31.5	-0.6	18 51 10	-01 31	18?	S?	2?	?	
31.9	+0.0	18 49 25	-00 55	7×5	S	25	varies	3C391
32.0	-4.9	19 06 00	-03 00	60?	S?	22?	0.5?	3C396.1
32.1	-0.9	18 53 10	-01 08	40?	C?	4?	0.7?	
32.4	+0.1	18 50 05	-00 25	6	S	0.8?	0.2?	
32.8	-0.1	18 51 25	-00 08	22×15	S?	12	0.3	Kes 78
33.2	-0.6	18 53 50	-00 02	18	S	3	0.3	
33.6	+0.1	18 52 48	+00 41	10	S	20	0.51	Kes 79, 4C00.70, HC13
34.7	-0.4	18 56 00	+01 22	35×27	C	240	0.37	W44, 3C392
35.6	-0.4	18 57 55	+02 13	15×11	S?	9	varies	
36.6	-0.7	19 00 35	+02 56	25?	S?	1.0	0.7?	
36.6	+2.6	18 48 49	+04 26	17×13?	S	0.7?	0.5?	
38.7	-1.3	19 06 40	+04 28	32×19?	S	?	?	
39.2	-0.3	19 04 08	+05 28	8×6	C	18	0.34	3C396, HC24, NRAO 593
39.7	-2.0	19 12 20	+04 55	120×60	?	85?	0.7?	W50, SS433
40.5	-0.5	19 07 10	+06 31	22	S	11	0.4	
41.1	-0.3	19 07 34	+07 08	4.5×2.5	S	25	0.50	3C397
41.5	+0.4	19 05 50	+07 46	10	S?	1?	?	
42.0	-0.1	19 08 10	+08 00	8	S?	0.5?	?	
42.8	+0.6	19 07 20	+09 05	24	S	3?	0.5?	
43.3	-0.2	19 11 08	+09 06	4×3	S	38	0.46	W49B
43.9	+1.6	19 05 50	+10 30	60?	S?	9.0	0.5	
45.7	-0.4	19 16 25	+11 09	22	S	4.2?	0.4?	
46.8	-0.3	19 18 10	+12 09	15	S	16	0.54	(HC30)
49.2	-0.7	19 23 50	+14 06	30	S?	160?	0.3?	(W51)

Table 1. (continued).

l l°	b b°	RA (J2000) /(h m s)	Dec /($^\circ$ ')	size /arcmin	type	Flux at 1 GHz/Jy	spectral index	other name(s)
53.4	+0.0	19 29 57	+18 10	10?	S	1.5	0.6?	
53.6	-2.2	19 38 50	+17 14	33×28	S	8	0.50	3C400.2, NRAO 611
54.1	+0.3	19 30 31	+18 52	12?	C?	0.5	0.1	
54.4	-0.3	19 33 20	+18 56	40	S	28	0.5	(HC40)
55.0	+0.3	19 32 00	+19 50	20×15?	S	0.5?	0.5?	
55.7	+3.4	19 21 20	+21 44	23	S	1?	0.3?	
57.2	+0.8	19 34 59	+21 57	12?	S?	1.8	0.35	(4C21.53)
59.5	+0.1	19 42 33	+23 35	15	S	3?	?	
63.7	+1.1	19 47 52	+27 45	8	F	1.8	0.24	
64.5	+0.9	19 50 25	+28 16	8	S?	0.15?	0.5	
65.1	+0.6	19 54 40	+28 35	90×50	S	5.5	0.61	
65.3	+5.7	19 33 00	+31 10	310×240	S?	42	0.6	
65.7	+1.2	19 52 10	+29 26	22	F	5.1	varies	DA 495
66.0	-0.0	19 57 50	+29 03	31×25?	S	?	?	
67.6	+0.9	19 57 45	+30 53	50×45?	S	?	?	
67.7	+1.8	19 54 32	+31 29	15×12	S	1.0	0.61	
67.8	+0.5	20 00 00	+30 51	7×5	?	?	?	
68.6	-1.2	20 08 40	+30 37	23	?	1.1	0.2	
69.0	+2.7	19 53 20	+32 55	80?	?	120?	varies	CTB 80
69.7	+1.0	20 02 40	+32 43	16×14	S	2.0	0.7	
70.0	-21.5	21 24 00	+19 23	330×240	S	?	?	
73.9	+0.9	20 14 15	+36 12	27	S?	9	0.23	
74.0	-8.5	20 51 00	+30 40	230×160	S	210	varies	Cygnus Loop
74.9	+1.2	20 16 02	+37 12	8×6	F	9	0.3	CTB 87
76.9	+1.0	20 22 20	+38 43	9	C	2?	?	
78.2	+2.1	20 20 50	+40 26	60	S	320	0.51	DR4, γ Cygni SNR
82.2	+5.3	20 19 00	+45 30	95×65	S	120?	0.5?	W63
83.0	-0.3	20 46 55	+42 52	9×7	S	1	0.4	
84.2	-0.8	20 53 20	+43 27	20×16	S	11	0.5	
85.4	+0.7	20 50 40	+45 22	24?	S	?	0.2	
85.9	-0.6	20 58 40	+44 53	24	S	?	0.2	
89.0	+4.7	20 45 00	+50 35	120×90	S	220	0.38	HB21
93.3	+6.9	20 52 25	+55 21	27×20	C?	9	0.45	DA 530, 4C(T)55.38.1
93.7	-0.2	21 29 20	+50 50	80	S	65	0.65	CTB 104A, DA 551
94.0	+1.0	21 24 50	+51 53	30×25	S	13	0.45	3C434.1
96.0	+2.0	21 30 30	+53 59	26	S	0.35	0.6	
106.3	+2.7	22 27 30	+60 50	60×24	C?	6	0.6	
107.0	+9.0	22 01 00	+66 30	180?	?	11?	0.9?	
108.2	-0.6	22 53 40	+58 50	70×54	S	8	0.5	
109.1	-1.0	23 01 35	+58 53	28	S	20	0.45	CTB 109
111.7	-2.1	23 23 26	+58 48	5	S	2300	0.77	Cassiopeia A, 3C461
113.0	+0.2	23 26 50	+61 26	40×17?	?	4	0.5?	
114.3	+0.3	23 37 00	+61 55	90×55	S	5.5	0.5	
116.5	+1.1	23 53 40	+63 15	80×60	S	10	0.5	
116.6	-26.1	00 23 00	+36 30	235	S	?	?	
116.9	+0.2	23 59 10	+62 26	34	S	8	0.57	CTB 1
119.5	+10.2	00 06 40	+72 45	90?	S	36	0.6	CTA 1
120.1	+1.4	00 25 18	+64 09	8	S	50	0.58	Tycho, 3C10, SN1572
126.2	+1.6	01 22 00	+64 15	70	S?	6	0.5	
127.1	+0.5	01 28 20	+63 10	45	S	12	0.45	R5
130.7	+3.1	02 05 41	+64 49	9×5	F	33	0.07	3C58, SN1181
132.7	+1.3	02 17 40	+62 45	80	S	45	0.6	HB3
150.3	+4.5	04 27 00	+55 28	180×150	S	?	?	
152.4	-2.1	04 07 50	+49 11	100×95	S	3.5?	0.7?	
156.2	+5.7	04 58 40	+51 50	110	S	5	0.5	

Table 1. (continued).

l /°	b /°	RA (J2000) /(h m s)	Dec /(° ′)	size /arcmin	type	Flux at 1 GHz/Jy	spectral index	other name(s)
159.6	+7.3	05 20 00	+50 00	240×180?	S	?	?	
160.9	+2.6	05 01 00	+46 40	140×120	S	110	0.64	HB9
166.0	+4.3	05 26 30	+42 56	55×35	S	7	0.37	VRO 42.05.01
178.2	-4.2	05 25 05	+28 11	72×62	S	2	0.5	
179.0	+2.6	05 53 40	+31 05	70	S?	7	0.4	
180.0	-1.7	05 39 00	+27 50	180	S	65	varies	S147
181.1	+9.5	06 26 40	+32 30	74	S	0.4?	0.4?	
182.4	+4.3	06 08 10	+29 00	50	S	0.5	0.4	
184.6	-5.8	05 34 31	+22 01	7×5	F	900	0.30	Crab Nebula, 3C144, SN1054
189.1	+3.0	06 17 00	+22 34	45	C	165	0.36	IC443, 3C157
189.6	+3.3	06 19 40	+22 00	90?	S	?	?	
190.9	-2.2	06 01 55	+18 24	70×60	S	1.3?	0.7?	
203.1	+6.6	06 57 00	+11 40	150	S	?	?	
205.5	+0.5	06 39 00	+06 30	220	S	140	0.4	Monoceros Nebula
206.7	+5.9	07 01 00	+08 10	210	S	?	?	
206.9	+2.3	06 48 40	+06 26	60×40	S?	6	0.5	PKS 0646+06
213.0	-0.6	06 50 50	-00 30	160×140?	S	21	0.4	
249.5	+24.5	09 34 00	-17 00	260	S	27	0.7	Hoinga
260.4	-3.4	08 22 10	-43 00	60×50	S	130	0.5	Puppis A, MSH 08-44
261.9	+5.5	09 04 20	-38 42	40×30	S	10?	0.4?	
263.9	-3.3	08 34 00	-45 50	255	C	1750	varies	Vela (XYZ)
266.2	-1.2	08 52 00	-46 20	120	S	50?	0.3?	RX J0852.0-4622
272.2	-3.2	09 06 50	-52 07	15?	S?	0.4	0.6	
279.0	+1.1	09 57 40	-53 15	95	S	30?	0.6?	
284.3	-1.8	10 18 15	-59 00	24?	S	11?	0.3?	MSH 10-53
286.5	-1.2	10 35 40	-59 42	26×6	S?	1.4?	?	
288.8	-6.3	10 30 20	-65 15	108×96	S	11	0.41	
289.7	-0.3	11 01 15	-60 18	18×14	S	6.2	0.2?	
290.1	-0.8	11 03 05	-60 56	19×14	S	42	0.4	MSH 11-61A
291.0	-0.1	11 11 54	-60 38	15×13	C	16	0.29	(MSH 11-62)
292.0	+1.8	11 24 36	-59 16	12×8	C	15	0.4	MSH 11-54
292.2	-0.5	11 19 20	-61 28	20×15	S	7	0.5	
293.8	+0.6	11 35 00	-60 54	20	C	5?	0.6?	
294.1	-0.0	11 36 10	-61 38	40	S	>2?	?	
296.1	-0.5	11 51 10	-62 34	37×25	S	8?	0.6?	
296.5	+10.0	12 09 40	-52 25	90×65	S	48	0.5	PKS 1209-51/52
296.7	-0.9	11 55 30	-63 08	15×8	S	3	0.5	
296.8	-0.3	11 58 30	-62 35	20×14	S	9	0.6	1156-62
298.5	-0.3	12 12 40	-62 52	5?	?	5?	0.4?	
298.6	-0.0	12 13 41	-62 37	12×9	S	5?	0.3	
299.2	-2.9	12 15 13	-65 30	18×11	S	0.5?	?	
299.6	-0.5	12 21 45	-63 09	13	S	1.0?	?	
301.4	-1.0	12 37 55	-63 49	37×23	S	2.1?	?	
302.3	+0.7	12 45 55	-62 08	17	S	5?	0.4?	
304.6	+0.1	13 05 59	-62 42	8	S	14	0.5	Kes 17
306.3	-0.9	13 21 50	-63 34	4	S?	0.16?	0.5?	
308.1	-0.7	13 37 37	-63 04	13	S	1.2?	?	
308.4	-1.4	13 41 30	-63 44	12×6?	S?	0.4?	?	
308.8	-0.1	13 42 30	-62 23	30×20?	C?	15?	0.4?	
309.2	-0.6	13 46 31	-62 54	15×12	S	7?	0.4?	
309.8	+0.0	13 50 30	-62 05	25×19	S	17	0.5	
310.6	-1.6	14 00 45	-63 26	2.5	C?	?	?	
310.6	-0.3	13 58 00	-62 09	8	S	5?	?	Kes 20B
310.8	-0.4	14 00 00	-62 17	12	S	6?	?	Kes 20A
311.5	-0.3	14 05 38	-61 58	5	S	3?	0.5	

Table 1. (continued).

l l°	b b°	RA (J2000) /(h m s)	Dec /($^\circ$ ')	size /arcmin	type	Flux at 1 GHz/Jy	spectral index	other name(s)
312.4	-0.4	14 13 00	-61 44	38	S	45	0.36	
312.5	-3.0	14 21 00	-64 12	20×18	S	3.5?	?	
315.1	+2.7	14 24 30	-57 50	190×150	S	?	?	
315.4	-2.3	14 43 00	-62 30	42	S	49	0.6	RCW 86, MSH 14-63
315.4	-0.3	14 35 55	-60 36	24×13	?	8	0.4	
315.9	-0.0	14 38 25	-60 11	25×14	S	0.8?	?	
316.3	-0.0	14 41 30	-60 00	29×14	S	20?	0.4	(MSH 14-57)
317.3	-0.2	14 49 40	-59 46	11	S	4.7?	?	
318.2	+0.1	14 54 50	-59 04	40×35	S	>3.9?	?	
318.9	+0.4	14 58 30	-58 29	30×14	C	4?	0.2?	
320.4	-1.2	15 14 30	-59 08	35	C	60?	0.4	MSH 15-52, RCW 89
320.6	-1.6	15 17 50	-59 16	60×30	S	?	?	
321.9	-1.1	15 23 45	-58 13	28	S	>3.4?	?	
321.9	-0.3	15 20 40	-57 34	31×23	S	13	0.3	
322.1	+0.0	15 20 49	-57 10	8×4.5?	S?	?	?	
322.5	-0.1	15 23 23	-57 06	15	C	1.5	0.4	
323.5	+0.1	15 28 42	-56 21	13	S	3?	0.4?	
323.7	-1.0	15 34 30	-57 12	51×38	S	?	?	
326.3	-1.8	15 53 00	-56 10	38	C	145	varies	MSH 15-56
327.1	-1.1	15 54 25	-55 09	18	C	7	?	
327.2	-0.1	15 50 55	-54 18	5	S	0.5	?	
327.4	+0.4	15 48 20	-53 49	21	S	26	0.6	Kes 27
327.4	+1.0	15 46 48	-53 20	14	S	1.9	?	
327.6	+14.6	15 02 50	-41 56	30	S	19	0.6	SN1006, PKS 1459-41
328.4	+0.2	15 55 30	-53 17	5	F	15	0.0	(MSH 15-57)
329.7	+0.4	16 01 20	-52 18	40×33	S	>34?	?	
330.0	+15.0	15 10 00	-40 00	180?	S	350?	0.5?	Lupus Loop
330.2	+1.0	16 01 06	-51 34	11	S?	5?	0.3	
332.0	+0.2	16 13 17	-50 53	12	S	8?	0.5	
332.4	-0.4	16 17 33	-51 02	10	S	28	0.5	RCW 103
332.4	+0.1	16 15 20	-50 42	15	S	26	0.5	MSH 16-51, Kes 32
332.5	-5.6	16 43 20	-54 30	35	S	2?	0.7?	
335.2	+0.1	16 27 45	-48 47	21	S	16	0.5	
336.7	+0.5	16 32 11	-47 19	14×10	S	6	0.5	
337.0	-0.1	16 35 57	-47 36	1.5	S	1.5	0.6?	(CTB 33)
337.2	-0.7	16 39 28	-47 51	6	S	1.5	0.4	
337.2	+0.1	16 35 55	-47 20	3×2	?	1.5?	?	
337.3	+1.0	16 32 39	-46 36	15×12	S	16	0.55	Kes 40
337.8	-0.1	16 39 01	-46 59	9×6	S	15	0.5	Kes 41
338.1	+0.4	16 37 59	-46 24	15?	S	4?	0.4	
338.3	-0.0	16 41 00	-46 34	8	C?	7?	?	
338.5	+0.1	16 41 09	-46 19	9	?	12?	?	
340.4	+0.4	16 46 31	-44 39	10×7	S	5	0.4	
340.6	+0.3	16 47 41	-44 34	6	S	5?	0.4?	
341.2	+0.9	16 47 35	-43 47	22×16	C	1.5?	0.6?	
341.9	-0.3	16 55 01	-44 01	7	S	2.5	0.5	
342.0	-0.2	16 54 50	-43 53	12×9	S	3.5?	0.4?	
342.1	+0.9	16 50 43	-43 04	10×9	S	0.5?	?	
343.0	-6.0	17 25 00	-46 30	250	S	?	?	RCW 114
343.1	-2.3	17 08 00	-44 16	32?	C?	8?	0.5?	
343.1	-0.7	17 00 25	-43 14	27×21	S	7.8	0.55	
344.7	-0.1	17 03 51	-41 42	8	C?	2.5?	0.3?	
345.1	-0.2	17 05 21	-41 26	6	S	1.4?	0.7?	
345.1	+0.2	17 03 40	-41 05	10	S	0.6?	0.6?	
345.7	-0.2	17 07 20	-40 53	6	S	0.6?	?	

Table 1. (continued).

l l°	b b°	RA (J2000) /(h m s)	Dec /($^\circ$ ')	size /arcmin	type	Flux at 1 GHz/Jy	spectral index	other name(s)
346.6	-0.2	17 10 19	-40 11	8	S	8?	0.5?	
347.3	-0.5	17 13 50	-39 45	65×55	S?	30?	?	RX J1713.7–3946
348.5	-0.0	17 15 26	-38 28	10?	S?	10?	0.4?	
348.5	+0.1	17 14 06	-38 32	15	S	72	0.3	CTB 37A
348.7	+0.3	17 13 55	-38 11	17?	S	26	0.3	CTB 37B
348.8	+1.1	17 11 29	-37 36	10	S	0.6?	0.7?	
349.2	-0.1	17 17 15	-38 04	9×6	S	1.4?	?	
349.7	+0.2	17 17 59	-37 26	2.5×2	S	20	0.5	
350.0	-2.0	17 27 50	-38 32	45	S	26	0.4	
350.1	-0.3	17 21 05	-37 27	4?	?	6?	0.8?	
351.0	-5.4	17 46 00	-39 25	30	S	?	?	
351.2	+0.1	17 22 27	-36 11	7	C?	5?	0.4	
351.7	+0.8	17 21 00	-35 27	18×14	S	10	0.5?	
351.9	-0.9	17 28 52	-36 16	12×9	S	1.8?	?	
352.7	-0.1	17 27 40	-35 07	8×6	S	4	0.6	
353.3	-1.1	17 33 10	-35 12	60	S	24?	0.85?	
353.6	-0.7	17 32 00	-34 44	30	S	2.5?	?	
353.9	-2.0	17 38 55	-35 11	13	S	1?	0.5?	
354.1	+0.1	17 30 28	-33 46	15×3?	C?	?	varies	
354.8	-0.8	17 36 00	-33 42	19	S	2.8?	?	
355.4	+0.7	17 31 20	-32 26	25	S	5?	?	
355.6	-0.0	17 35 16	-32 38	8×6	S	3?	?	
355.9	-2.5	17 45 53	-33 43	13	S	8	0.5	
356.2	+4.5	17 19 00	-29 40	25	S	4	0.7	
356.3	-1.5	17 42 35	-32 52	20×15	S	3?	?	
356.3	-0.3	17 37 56	-32 16	11×7	S	3?	?	
357.7	-0.1	17 40 29	-30 58	8×3?	?	37	0.4	MSH 17–39
357.7	+0.3	17 38 35	-30 44	24	S	10	0.4?	
358.0	+3.8	17 26 00	-28 36	38	S	1.5?	?	
358.1	+1.0	17 37 00	-29 59	20	S	2?	?	
358.5	-0.9	17 46 10	-30 40	17	S	4?	?	
359.0	-0.9	17 46 50	-30 16	23	S	23	0.5	
359.1	-0.5	17 45 30	-29 57	24	S	14	0.4?	
359.1	+0.9	17 39 36	-29 11	12×11	S	2?	?	
359.2	-1.1	17 48 14	-30 12	5×4	S?	0.4?	1.1?	